

Multimodal Rumor Detection Enhanced by External Evidence and Forgery Features

Han Li^{1,a} Hua Sun^{*}

¹ *Information Engineering School of Dalian Ocean University*

Dalian 116023, Liaoning, China

^a*Email: lihanhenku20011115@163.com*

^{*}*Information Engineering School of Dalian Ocean University*

Dalian 116023, Liaoning, China

Email: sunhua@dlou.edu.cn

Abstract

Social media increasingly disseminates information through mixed image–text posts, but rumors often exploit subtle inconsistencies and forged content, making detection based solely on post content difficult. Deep semantic-mismatch rumors, which superficially align images and texts, pose particular challenges and threaten online public opinion. Existing multimodal rumor detection methods improve cross-modal modeling but suffer from limited feature extraction, noisy alignment, and inflexible fusion strategies, while ignoring external factual evidence necessary for verifying complex rumors.

To address these limitations, we propose a multimodal rumor detection model enhanced with external evidence and forgery features. The model uses a ResNet34 visual encoder, a BERT text encoder, and a forgery-feature module extracting frequency-domain traces and compression artifacts via Fourier transformation. BLIP-generated image descriptions bridge image and text semantic spaces. A dual contrastive learning module computes contrastive losses between text–image and text–description pairs, improving detection of semantic inconsistencies. A gated adaptive feature-scaling fusion mechanism dynamically adjusts multimodal fusion and reduces redundancy.

Experiments on Weibo and Twitter datasets demonstrate that our model outperforms mainstream baselines in macro accuracy, recall, and F1 score.

Keywords: Multimodal rumor detection; image–text semantic matching; modality fusion; attention mechanism; image forgery

1 Introduction

The rapid development of social networks enables various types of information to be widely disseminated within a very short period of time, which brings convenience to users while also providing favorable conditions for the generation and spread of false content. Driven by the traffic economy, online rumors have significantly improved in content breadth, dissemination speed, update frequency, and scope of influence, severely undermining online order and social trust. For example, in recent special rectification campaigns, relevant authorities have handled a large number of illegal accounts and rumor-related information according to law, highlighting the urgency of rumor governance in the social network environment. Meanwhile, with the diversification of communication forms, posts on social platforms are often accompanied by images, and rumor makers frequently combine real or synthetic images with false text, forming more deceptive image–text combinations [1]. Therefore, authenticity detection for multimodal posts on social networks, in order to achieve accurate rumor identification, has become a current research hotspot. Existing multimodal rumor detection

models mostly crawl posts from social platforms, extract features of modalities such as text and images, and fuse them to classify rumors. Although researchers have developed various models, several common issues remain. In the image-modality feature extraction stage, most studies focus on spatial-domain features [2] but ignore tampering traces in the frequency domain [3]. Although image-text consistency is often used as a judgment basis, the calculation of this consistency and its role in model decision-making are often unclear [4]. In terms of integrating social contextual features, due to the lack of explicit modeling of the post-comment-user interaction structure, models struggle to capture dissemination characteristics. Because structural noise widely exists in social network graphs, traditional graph neural networks easily learn misleading contextual features, affecting detection reliability. The feature extraction stage often relies on a single extraction method, resulting in insufficient mining of intra-modality heterogeneity. In the fusion stage, some methods only adopt simple concatenation and fail to handle semantic differences between modalities; although attention mechanisms are used, their usage methods and feature coverage remain limited [5].

To address the above challenges, this paper proposes a multimodal rumor detection framework that integrates forgery-feature extraction, dual contrastive semantic alignment, and a gated fusion mechanism. In the visual branch, we design a forgery-feature extraction module based on Fourier transformation to capture potential image tampering traces. At the semantic level, we construct a dual contrastive mechanism that includes contrast between text and images as well as contrast between text and image descriptions, thereby reinforcing semantic alignment and suppressing the risk of noisy alignment. To address fluctuations in evidence quantity and modality noise, we design a gated modulation module that dynamically controls the multimodal feature fusion process through a learnable gating function combined with an adaptive feature-scaling mechanism, thereby improving control over modality flows and enhancing model robustness. Experimental results conducted on MR2 show that factors such as evidence quantity and forgery features significantly affect detection performance.

Overall, the main contributions of this paper include:

- (1) proposing a detection framework that integrates forgery features with cross-modal semantic features to address both semantic manipulation and visual-tampering attacks;
- (2) designing a gated fusion mechanism to achieve dynamic fusion of multimodal features and redundancy suppression;
- (3) Systematic experiments on multimodal rumor datasets demonstrate that the proposed method achieves an improvement in macro-accuracy compared to baseline methods.

2 Related Work

2.1 Monomodal Rumor Detection

Research on rumor and fake-news detection in social media has formed a multidimensional technical system, evolving from traditional machine learning relying on handcrafted features, to deep-learning sequence modeling, graph-structure mining, multimodal fusion, and finally to recent advances leveraging large language models (LLMs) and reinforcement learning. Existing monomodal rumor detection methods utilize features extracted from either text or images to detect rumors. Early rumor detection studies mainly focused on mining prominent features in the rumor propagation process and applied traditional machine-learning

classifiers for identification. Kwon et al. [6] conducted an in-depth study on the temporal, structural, and linguistic characteristics of rumor propagation, proposing a periodic external-shock model to capture the cyclical outbreak features of rumors over time. They also found that isolated nodes have a higher proportion in rumor propagation networks, and that the frequency of negation words in rumor content is significantly higher than in non-rumor content. These studies provided important feature foundations for subsequent deep-learning models.

To overcome the limitations of handcrafted features, researchers began using models such as recurrent neural networks (RNNs) to automatically learn high-dimensional features. Ma et al. [7] first applied RNNs to capture temporal variation features of tweet content. On this basis, Chen et al. [8] proposed the dARNN model, which employs a GRU with a deep attention mechanism (a variant of recurrent neural networks) to capture long-range dependencies in post sequences, thereby enabling the model to filter out highly discriminative key clues from the highly redundant early information. In addition, Alkhodair et al. [9] combined Word2Vec with LSTM to learn semantic features of text content, detecting sudden-news rumors related to emerging topics. Luvembe et al. [10] proposed a deep-normalization-based attention mechanism to extract dual emotional features of rumors. Moreover, to achieve near-real-time source blocking, Xu et al. [11] proposed a topic-driven rumor detection framework (TDRD), which uses LDA to extract the topic distribution vector of the source microblog and combines it with content features extracted by a CNN. The study verifies that the importance and ambiguity of topics are key factors in the emergence of rumors, thereby enabling early near-real-time detection that relies solely on the source post without depending on subsequent interactions.

With the prevalence of multimedia content, relying solely on textual features is insufficient to cope with complex falsification methods. Cao et al. [12] systematically reviewed the role of visual content in fake news, categorizing it into forensic features, semantic features, statistical features, and contextual features. Qi et al. [13] proposed a multi-domain visual neural network (MVNN), which captures physical manipulation traces of images through a frequency-domain subnetwork, combines them with semantic features captured by a pixel-domain subnetwork, and uses an attention mechanism to integrate textual information for multimodal classification. This study strongly demonstrates the high complementarity between frequency-domain and pixel-domain features in identifying different types of fake-news images. Recently, the application of large language models (LLMs) in rumor detection has become a research hotspot. Huang et al. [14] proposed the FakeGPT framework, systematically evaluating ChatGPT's capabilities in rumor generation, explanation, and detection, and introduced causality-aware prompts. Zhang and Gao [15], aiming at the reasoning deficiencies of LLMs in complex fact-checking, proposed a hierarchical step-by-step prompting method (HiSS). This method guides the LLM to decompose a complex news claim into multiple sub-claims and verifies them one by one through hierarchical question-answering (QA) steps, significantly improving the accuracy of fact-checking and providing fine-grained logical interpretability for the final judgment.

2.2 Multimodal Rumor Detection

With the evolution of the social media ecosystem, the forms of rumor propagation have shifted from single-text to multimodal formats that include images and videos, which has

driven researchers to leverage cross-modal complementarity to enhance detection performance. Early work mainly focused on multimodal feature extraction and fusion. Wang et al. [16] proposed the EANN model, which uses adversarial neural networks to extract textual and visual features and employs an event discriminator to remove dependencies on specific events, thereby learning more generalizable feature representations. Nguyen et al. [17] introduced a deep Markov random field, using inter-article correlations to assist judgment. In addition, Kirchknopf et al. [18] proposed a multi-stream architecture that not only fuses textual and visual content but also incorporates user comments and metadata, further improving detection accuracy through a hierarchical fusion strategy.

As research progressed, simple feature concatenation was gradually replaced by more sophisticated interaction mechanisms. For example, Luvembe et al. [19] proposed the CAF-ODNN model, which introduces a Complementary Attention Fusion (CAF) mechanism to directly capture fine-grained cross-modal correlations between text and images at the feature level. This method effectively filters out irrelevant semantic noise and, combined with a grid search optimization strategy, significantly improves the accuracy of multimodal fake news detection. Liu et al. [20] proposed MVACLNet, which addresses the lack of diversity in feature space through virtual augmented contrastive learning.

Beyond feature fusion, researchers have increasingly recognized that image–text inconsistency or semantic conflict is a key cue for rumor identification, giving rise to consistency-based detection methods. The SAFE model proposed by Zhou et al. [21] captures cross-modal mismatches by calculating similarity between textual and visual features. Xue et al. [22] proposed a multimodal consistency exploration framework. On the basis of capturing the semantic consistency between text and images, the model further introduces the SRM filter to extract the physical statistical features of images, and significantly improves the capability of identifying high-quality forged images by detecting physical tampering traces such as synthesis and modification. Abdelnabi et al. [23] proposed the CCN network, which targets “out-of-context” fake news by retrieving external evidence from the open web and performing multi-dimensional consistency checking using features extracted by CLIP. However, Zhang et al. [24], through large-scale data analysis, challenged the traditional assumption that image–text inconsistency implies falsehood, pointing out that rumor makers often deliberately select highly matched images to increase deception, providing a new perspective for similarity-based detection methods.

Although the above methods have achieved significant progress in feature mining and consistency detection, most rely solely on the content of the posts themselves and lack support from external knowledge, resulting in misjudgments when facing carefully fabricated rumors. Therefore, introducing external evidence for reasoning has become a cutting-edge research trend and constitutes the focus of this paper. Wu et al. [25] constructed the Chinese multimodal rumor dataset CSMRE containing evidence and proposed the EAMRD model, which fuses multimodal features with retrieved evidence using a cross-attention mechanism. To address the model’s tendency to capture false correlations, Wu et al. [26] designed the ERD-DC model, which adopts a dual-channel strategy: using factual evidence to quickly detect old rumors while employing multi-dimensional features to detect new rumors, effectively balancing efficiency and accuracy. In addition, Huang et al. [27] proposed the DEETSA model, which combines dual evidence enhancement with image–text similarity

perception and achieves efficient fusion of multi-source information through an adaptive gated network.

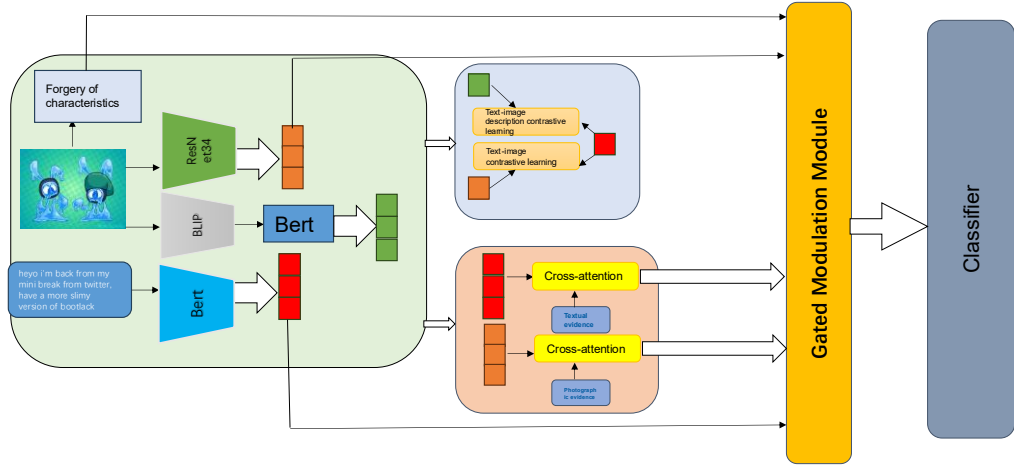


Figure 1. Model Structure Diagram

3 Methodology

This paper proposes a multimodal rumor detection model enhanced by external evidence and forgery features. Our model consists of four modules: the feature encoding module, the dual contrastive semantic alignment module, the evidence fusion module, and the gated modulation module. The interaction of these modules enables the model to fully extract and integrate valuable features from complex multimodal information, thereby enhancing overall performance. This section provides a detailed explanation of the proposed framework, as shown in Figure 1.

3.1 Feature Extraction

In the multimodal rumor detection task, images and texts, as the two input modalities, differ not only in expression forms but also in information structure and semantic representation. To effectively extract meaningful features from these two modalities, the feature extraction module must be capable of deeply mining latent information in images and texts and mapping them into a unified feature space. This module combines image feature extraction, text feature encoding, and forgery-feature extraction, and enhances the alignment capability between images and texts through an effective fusion method.

3.1.1 Text Features

Text features are encoded using the BERT model. The BERT model, through a bidirectional Transformer encoder, is able to capture rich semantic information from context. After the textual data is input to BERT, the model learns representations of each word in context through its deep network. The goal of text feature encoding is to transform the original text into a high-dimensional semantic vector, which not only contains the specific meaning of words but also captures contextual relationships between words, thereby enabling learning of key information relevant to images, as follows:

$$h_T = \text{BERT}(T)$$

where T represents the input textual information, $h_T \in \mathbb{R}^{d_T}$ denotes the text feature, and d_T is the feature dimension.

3.1.2 Image Features

Image features are encoded using the ResNet34 network. ResNet34 is a deep residual network that addresses the gradient vanishing problem in deep neural networks through residual blocks, allowing the network to handle deeper structures. This model is capable of extracting high-dimensional visual features from images and learning key information contained in them, as follows:

$$h_I = \text{ResNet34}(I)$$

where I denotes the input image information, $h_I \in \mathbb{R}^{d_I}$ represents the image feature, and d_I is the feature dimension.

3.1.3 Forgery Feature Extraction

To further enhance the model's ability to recognize forgery content in images, this paper designs a forgery-feature extraction module based on Fourier transformation and low-frequency features. This module extracts discriminative forgery features through frequency-domain transformation, multi-scale convolutional sampling, and global-dependency modeling.

Given a color image X of size $H \times W$, for each color channel, its two-dimensional discrete Fourier transform produces a complex spectrum X_{comp} . At the point (u, v) , the computation is defined as:

$$X_{\text{comp}}(u, v) = \sum_{m=0}^{H-1} \sum_{n=0}^{W-1} X(m, n) \cdot e^{-j2\pi(\frac{um}{H} + \frac{vn}{W})}$$

where $X(m, n)$ is the pixel value at coordinate (m, n) in the spatial domain. $X_{\text{comp}}(u, v)$ is the complex value in the frequency domain at coordinate (u, v) , representing the component of the wave with frequency u and v in the original image. According to Euler's formula $e^{j\theta} = \cos \theta + j \sin \theta (j^2 = -1)$, pixel values can be decomposed into a combination of sine and cosine waves.

A complex number contains a real part and an imaginary part, which cannot be directly processed by convolutional layers. Therefore, the amplitude spectrum $M(u, v)$ is calculated, representing the energy magnitude of each frequency component:

$$M(u, v) = |X_{\text{comp}}(u, v)| = \sqrt{\text{Re}(X_{\text{comp}}(u, v))^2 + \text{Im}(X_{\text{comp}}(u, v))^2}$$

where Re and Im denote the real and imaginary parts of the complex number, respectively. Since the values of $M(u, v)$ vary widely, directly inputting them into a neural network may cause gradient instability. Therefore, compression is applied:

$$X_{\text{feat}}(u, v) = \ln(1 + M(u, v))$$

Next, the low-frequency region is cropped to filter out random noise:

$$X_{\text{freq}} = \{X_{\text{feat}}(u, v) \mid (u, v) \in \Omega\}$$

where Ω corresponds to the central 128×128 low-frequency energy region of the spectrum, which concentrates the main structural information of the image.

Then, X_{freq} is input to a backbone network, and low-level features are extracted through convolutional layers:

$$F_{\text{backbone}} = \text{CNN}(X_{\text{freq}})$$

where CNN denotes a convolutional neural network, and the output F_{backbone} represents the initial image features.

Next, multi-scale features are obtained using different convolution kernels ($1 \times 1, 3 \times 3, 5 \times 5$) and pooling operations, and the outputs are concatenated:

$$F_{\text{ms}} = [F_{\text{branch1}}, F_{\text{branch3}}, F_{\text{branch5}}, F_{\text{branch_pool}}]$$

To model long-range frequency dependencies across different image regions, the module introduces a multi-head self-attention mechanism. F_{ms} is reshaped and transposed into a sequence $Z \in \mathbb{R}^{L \times C}$, where $L = H' \times W'$, C is the number of feature channels, and $H' \times W'$ is the height and width of the feature map.

For the i -th attention head, the computation is:

$$\text{Attention}(Q_i, K_i, V_i) = \text{softmax}\left(\frac{Q_i K_i^T}{\sqrt{d_k}}\right) V_i$$

where Q, K, V are the queries, keys, and values obtained from Z via linear projection, and

$\sqrt{d_k}$ is a scaling factor used to prevent large dot products from causing gradient vanishing.

By concatenating the outputs of N heads and applying a linear projection, an enhanced feature sequence is obtained. Finally, global average pooling (GAP) followed by a fully connected (FC) layer generates the final forgery feature vector:

$$h_{\text{forgery}} = \text{FC}(\text{GAP}(\text{MultiHead}(Z)))$$

3.2 Evidence Fusion Module

To enhance semantic consistency across modalities through contrastive learning between text and evidence, as well as image and evidence, this paper introduces a multi-head attention-based evidence fusion module, inspired by the work of Huang et al. [27].

For textual evidence, we weight the evidence using a multi-head attention mechanism, allowing the selection of relevant evidence based on the main text features. Specifically, given the main text feature h_T as the query, and the textual evidence \tilde{E}_t as keys and values, multi-head attention is computed as follows. First, the main text feature h_T is mapped to a query vector, and the textual evidence features \tilde{E}_t , obtained from BERT, are mapped to key and value vectors:

$$Q = h_T W^Q, K = \tilde{E}_t W^K, V = \tilde{E}_t W^V$$

where W^Q, W^K, W^V are learnable weight matrices.

To capture the relevance between the main text and evidence, the output of the i -th attention head head_i is calculated as:

$$\text{head}_i = \text{Attention}(Q_i, K_i, V_i) = \text{softmax}\left(\frac{Q_i K_i^T}{\sqrt{d_k}}\right) V_i$$

All head outputs are then concatenated and passed through a linear transformation to obtain the final attention-weighted evidence feature H_a . The fused textual feature is denoted as H'_T :

$$H'_T = \text{MultiHeadAttn}(Q = h_T, K = \tilde{E}_t, V = \tilde{E}_t)$$

The processing of image evidence is similar to textual evidence. The image feature h_I is used as the query, and the image evidence \tilde{E}_i , obtained by ResNet34, is used as keys and values:

$$H'_I = \text{MultiHeadAttn}(Q = h_I, K = \tilde{E}_i, V = \tilde{E}_i)$$

By integrating external evidence, the model can effectively align across multiple modalities and evidence, ensuring that it focuses on relevant evidence when processing multimodal

information, thereby improving the accuracy of rumor detection.

3.3 Dual-Contrast Perception Module

To enhance the model's ability to identify rumors with semantic mismatches between text and images, this paper designs a dual-contrast similarity perception mechanism. This mechanism consists of two complementary contrastive learning objectives: semantic alignment between text and image descriptions, and semantic alignment between text and visual image features. These two types of alignment constrain the consistency of the feature space at the semantic and visual levels, respectively, thereby improving the model's comprehensive perception of text-image relationships. In particular, it can effectively detect rumors when there is surface-level mismatch between image descriptions and text.

3.3.1 Image Description Generation and Semantic Mapping

Unlike traditional methods that directly compute similarity in the visual feature space, this paper uses the BLIP [28] model to generate descriptive texts for images, converting visual features into interpretable textual semantic representations. Similar methods have also been used in [27] and achieved notable results.

Let the original image be I . After processing with the BLIP model, the corresponding textual description is $\text{BLIP}(I)$. The semantic feature e_t is then extracted using BERT, as follows:

$$e_t = \text{BERT}(\text{BLIP}(I))$$

3.3.2 Text–Image Description Semantic Alignment

We first compute the semantic similarity between the original text feature h_T and the BLIP-generated image description feature e_t .

Define normalized features u and v . In a batch of size N , the similarity matrix between all texts and all image descriptions is M_{tt} , where the element in the i -th row and j -th column, $s_{i,j}$, represents the similarity between the i -th text and the j -th image description:

$$s_{i,j} = u_i \cdot v_j^\top$$

To train the model to recognize consistency, the similarity of positive pairs on the diagonal should be maximized while the similarity of negative pairs off the diagonal should be minimized.

For the i -th sample, the InfoNCE loss is defined as:

$$L_{TT} = -\log \frac{\exp(s_{i,i}/\tau)}{\sum_{j=1}^N \exp(s_{i,j}/\tau)}$$

where $s_{i,i}$ is the score of the positive pair between the current text and its corresponding image description, $s_{i,j} (i \neq j)$ are negative pair scores, and τ is the temperature parameter used to adjust sensitivity to hard negatives.

This loss reinforces the consistency between image content and text descriptions at the semantic level by maximizing the similarity of matching samples ($i = j$) and minimizing the similarity of non-matching samples ($i \neq j$). It effectively detects semantic-level contradictions, for example, when the event described in text does not match the visual scene in the image.

3.3.3 Text–Image Visual Alignment

To ensure semantic coherence at the visual level, the InfoNCE loss for the i -th sample is defined as:

$$L_{TI} = -\log \frac{\exp(s_{i,i}^i/\tau)}{\sum_{j=1}^N \exp(s_{i,j}^i/\tau)}$$

$$s_{i,j}^i = \mathbf{u}_i \cdot \mathbf{g}_j^T$$

where $s_{i,j}^i$ represents the similarity between the i -th text and the j -th image, and \mathbf{u} and \mathbf{g} denote the normalized text and image features, respectively.

3.3.4 Joint Optimization of Dual Contrast

The overall objective of the similarity perception module is:

$$\mathcal{L}_{\text{sim}} = \lambda_{TT} L_{TT} + \lambda_{TI} L_{TI}$$

where λ_{TT} and λ_{TI} are balancing coefficients for semantic alignment and visual alignment, respectively.

Through dual-contrast constraints, the model simultaneously learns semantic-level alignment, ensuring consistency between textual descriptions and image content, and visual-level alignment, strengthening the correspondence between text and images in appearance and entities. This semantic-visual dual constraint allows the model to capture subtle cross-modal inconsistencies when encountering mismatched images and text or misleading headlines, thereby significantly improving detection accuracy.

3.4 Gated Modulation Module

In multimodal rumor detection tasks, text and images often exhibit high complexity and uncertainty at the semantic level. Due to the heterogeneous information sources and substantial differences in semantic expression, directly performing feature concatenation or weighted fusion may easily cause semantic conflicts and feature redundancy. Traditional fusion methods usually employ static weighting or simple concatenation, which cannot adaptively adjust the fusion ratio between modalities according to contextual semantic relationships, resulting in inflexible and non-selective feature representation. Different modal features may differ significantly in numerical scale and activation intensity, and directly using them for classification may lead to feature amplification or unstable training.

To address this, an adaptive feature-scaling mechanism is introduced to constrain the overall scale of fused features. Based on this, the paper proposes a gated modulation module that combines the gating mechanism with adaptive feature scaling for fine-grained feature fusion modeling and coarse-grained feature magnitude modulation.

3.4.1 Gated Modulation Mechanism

During the fusion stage, the model applies hierarchical gating control to text and image features to determine the contribution ratio of the main post information and external evidence. Specifically, let the main post text feature be $\mathbf{h}_T, \mathbf{h}_T \in \mathbb{R}^{d_T}$, and the text feature enhanced by evidence attention be $\tilde{\mathbf{h}}_T, \tilde{\mathbf{h}}_T \in \mathbb{R}^{d_T}$. Let the main post image feature be $\mathbf{h}_I, \mathbf{h}_I \in \mathbb{R}^{d_I}$, and the image feature enhanced by evidence attention be $\tilde{\mathbf{h}}_I, \tilde{\mathbf{h}}_I \in \mathbb{R}^{d_I}$.

The model first concatenates the two features and applies a linear transformation followed by a Sigmoid activation to obtain the inter-modal gating weights:

$$\alpha_T = \sigma(W_T[\mathbf{h}_T; \tilde{\mathbf{h}}_T]), \quad \alpha_I = \sigma(W_I[\mathbf{h}_I; \tilde{\mathbf{h}}_I])$$

where $\sigma(\cdot)$ denotes the Sigmoid function, and W_T, W_I are learnable parameter matrices.

Then, the model performs weighted fusion of the main post and evidence features according to the gating coefficients:

$$h_T^{\text{fusion}} = \alpha_T \cdot \mathbf{h}_T + (1 - \alpha_T) \cdot \tilde{\mathbf{h}}_T, \quad h_I^{\text{fusion}} = \alpha_I \cdot \mathbf{h}_I + (1 - \alpha_I) \cdot \tilde{\mathbf{h}}_I$$

The gating weights α_T and α_I reflect the importance of different modal features. When the main post information is sufficient, the gating factor tends to increase, allowing the model to retain more of the original semantics. When the external evidence contains strongly relevant

or contradictory information, the gating coefficients decrease, enabling the model to actively incorporate external information for semantic correction.

3.4.2 Cross-Modal Gated Fusion

After completing the single-modal gating, the model further fuses text and image semantic features in the cross-modal space. The gated text feature h_T^{fusion} and image feature h_I^{fusion} are mapped into the same latent space:

$$h'_T = W_C h_T^{\text{fusion}}, \quad h'_I = W_I h_I^{\text{fusion}}$$

Then, a second-layer gating structure implements interaction fusion between the two modalities:

$$\beta = \sigma(W_{TI}[h'_T; h'_I]), \quad h_{TI}^{\text{fusion}} = \beta \cdot h'_T + (1 - \beta) \cdot h'_I$$

where β denotes the cross-modal gating weight, controlling the proportion of text and image in the fused features.

Finally, forgery features are integrated to enhance the model's ability to recognize image manipulation:

$$h_{\text{forgery}} = W_s h_{\text{forgery}}, \quad h_{\text{final}} = \gamma \cdot h_{TI}^{\text{fusion}} + (1 - \gamma) \cdot h_{\text{forgery}}$$

Where $\gamma = \sigma(W_h[h_{TI}^{\text{fusion}}; h_{\text{forgery}}])$, $h_{\text{forgery}} \in \mathbb{R}^f$, $h_{\text{final}} \in \mathbb{R}^f$.

3.4.3 Adaptive Feature Scaling Mechanism

After obtaining the fused features, the model introduces an adaptive feature scaling mechanism to further improve robustness. This mechanism modulates the fused features through a learnable scaling parameter λ :

$$h_{\text{final}} = \lambda \cdot h_{\text{final}}, \quad \lambda \in (0,1]$$

This gating parameter is jointly optimized with the other model parameters during training and is used to adaptively control the overall strength of the fused features. As a result, it mitigates noise interference caused by the accumulation of multimodal features and enhances the stability and generalization ability of the model during training.

3.5 Classifier Design

This study constructs a classification prediction module based on a two-layer perceptron, aiming to perform final category discrimination on the multimodal comprehensive feature h_{final} obtained after gated fusion and adaptive feature scaling. This feature vector deeply integrates and enhances text semantics, image content, and forgery features, providing solid evidence for authenticity determination.

In implementation, the classifier first maps the fused features to a high-dimensional space through the first fully connected layer FC_1 , embedding a LeakyReLU activation function to alleviate the “dead neuron” problem in deep networks and ensure continuous effective gradient flow during model iterations. The second fully connected layer FC_2 then maps the feature to a category prediction space of dimension C , outputting unnormalized logit vector h_{class} . Finally, the model applies the Softmax function to convert this vector into a predicted probability distribution y .

$$h_{\text{class}} = FC_2(\text{LeakyReLU}(FC_1(h_{\text{final}}))), \quad y = \text{Softmax}(h_{\text{class}})$$

where y denotes the output probability distribution of the classifier.

The classifier is trained using the cross-entropy loss, which is commonly employed in classification tasks. The cross-entropy loss measures the difference between the predicted distribution and the ground-truth label distribution. For single-sample classification, the loss is defined as:

$$\mathcal{L}_{\text{class}} = - \sum_{i=1}^C p_i \log (q_i)$$

where C is the number of classes, p_i is the ground-truth probability for class i , and q_i is the predicted probability for class i .

4. Experiments

In this section, we provide a detailed description of the experiments conducted to validate the performance of the proposed method. First, the two experimental datasets, Twitter and Weibo, are described. Next, we introduce the specific experimental settings and evaluation metrics. Subsequently, experimental results are presented and analyzed, including hyperparameter studies, comparisons with state-of-the-art methods, ablation studies, and error analysis. Finally, a case study is conducted to intuitively demonstrate the advantages and limitations of our method.

4.1 Datasets

This study uses the MR2 dataset, released by Hu et al. [29], which is specifically designed for multimodal rumor detection. MR2 consists of two sub-datasets from Twitter and Weibo, covering content from English and Chinese social media platforms. Each sample contains a text paragraph and an accompanying image. The samples are labeled into three categories: rumor, non-rumor, and unconfirmed rumor.

The construction of the MR2 dataset not only involves collecting text–image pairs but also retrieving additional textual and visual evidence from the web. Image evidence is typically obtained through reverse image search of the original image, while textual evidence is acquired by searching the original text to collect relevant web page titles, summaries, and other textual information.

4.2 Experimental Settings and Evaluation Metrics

In this experiment, the dataset is split into training, validation, and test sets with a ratio of 8:1:1. The maximum text length is set to 40 tokens to accommodate most Twitter and Weibo samples. In practice, the maximum number of text and visual evidence items for each post is set to 5, and 8 attention heads are used for cross-attention.

The classification task employs a two-layer perceptron network. During training, the model uses the AdamW optimizer with an initial learning rate of 5×10^{-5} , a batch size of 32, and a total of 8 training epochs. Learning rate adjustment is performed using the ExponentialLR scheduler to dynamically tune the learning rate and improve training efficiency.

To prevent overfitting, an early stopping strategy with a patience of 2 is employed, meaning training stops when validation performance no longer improves. The method is implemented based on the PyTorch deep learning framework. Macro Accuracy (M_ACC), Precision (PRE), Recall (REC), and F1-score (F1) are adopted as the main evaluation metrics to comprehensively assess the model's performance in rumor detection tasks.

4.3 Experimental Results and Analysis

4.3.1 Effect of Evidence Quantity

The maximum number of evidence items is a key hyperparameter. Too few pieces of evidence may provide insufficient information for effective reasoning, while too many may introduce irrelevant or erroneous noise. We gradually adjusted the maximum number of retrieved textual and visual evidence items from 1 to 9 and observed the changes in macro accuracy

on the Weibo and Twitter datasets, as shown in Figure 2.

The experimental results indicate that the optimal number of evidence items for both Weibo and Twitter is 5. The quality and quantity of the retrieved textual and visual evidence significantly influence the model's performance. Insufficient evidence fails to provide adequate explanatory information for the original post, reducing the effectiveness of rumor detection. Conversely, excessive evidence can introduce erroneous information and noise, which negatively affects model performance.

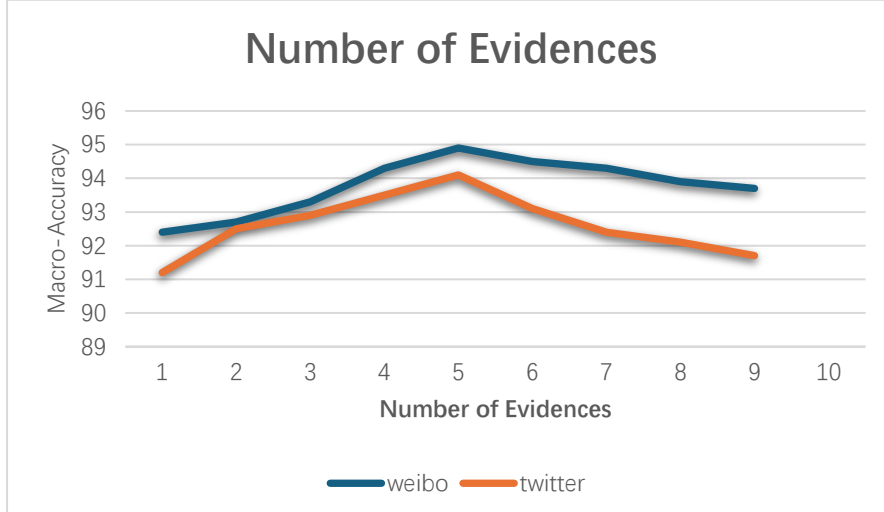


Figure 2

4.3.2 Comparison with Baseline Methods

To validate the effectiveness of the proposed method, we six the following seven approaches as comparison baselines:

1. CLIP [30]: Uses the image encoder of CLIP to extract image features, and classifies the feature vector corresponding to the special token “CLS” via a linear layer.
2. LSTM_word2vec [9]: A text-only detection method. It employs word2vec and LSTM to extract semantic features from text content for rumor detection.
3. DEDA [10]: A text-only detection method. It utilizes a deep normalized attention mechanism to extract sentiment features from text for rumor judgment.
4. MTTV [31]: A multimodal detection method. It leverages a multimodal transformer to integrate semantic information from images and text, where image features are processed using a two-level visual feature extraction scheme.
5. HMCAN [32]: A multimodal detection method. It employs a hierarchical multimodal context attention network (HMCAN) to model contextual information in both text and images for rumor detection.
6. CCN [23]: A multimodal detection method specifically designed to address the selective distortion problem in text–image mismatches. It uses a Consistency Checking Network (CCN) to learn and determine whether external evidence is consistent with post content.

Weibo

table 1

non

rumor

unver

	Acc	prec	rec	F1	prec	rec	F1	prec	rec	F1
CLIP	82.8	88.7	90.3	89.5	87.2	75.6	81.0	78.2	82.5	80.3
LSTM_Word2vec	86.3	90.5	91.6	91.1	82.8	78.1	80.4	87.5	89.3	88.4
DEDA	88.6	93.6	93.4	93.5	84.6	81.5	83.0	89.1	90.9	90.0
HMCAN	89.7	95.9	94.2	95.0	86.1	82.6	84.3	89.4	92.3	90.8
MTTV	90.8	95.2	94.5	94.9	86.5	85.4	86.0	91.5	92.6	92.1
CCN	92.0	96.7	95.5	96.1	85.7	87.9	86.8	93.9	93.5	93.7
ours	94.9	95.1	96.3	95.7	88.6	96.1	92.2	97.3	92.3	94.7

Twitter table 2

	non				rumor				unver		
	Acc	prec	rec	F1	prec	rec	F1	prec	rec	F1	
CLIP	83.8	92.6	85.3	88.8	81.3	79.8	80.5	81.1	86.3	83.6	
LSTM_Word2vec	87.0	89.6	91.8	90.7	82.4	76.8	79.5	91.2	92.4	91.8	
DEDA	88.8	91.9	93.4	92.6	84.9	79.5	82.1	91.8	93.4	92.6	
HMCAN	89.9	92.9	93.7	93.3	85.4	82.2	83.8	92.8	93.8	93.3	
MTTV	90.1	93.6	94.4	94.0	85.6	81.8	83.7	92.9	94.2	93.5	
CCN	91.8	94.8	95.7	95.2	88.7	84.5	86.5	93.8	95.2	94.5	
ours	94.1	97.9	95.5	96.7	85.5	91.5	88.4	96.8	95.4	96.1	

Tables 1 and 2 present a detailed comparison of the proposed method with the seven baseline approaches on the Weibo and Twitter datasets. Overall, our model demonstrates significant superiority across all evaluation metrics on both datasets, confirming its effectiveness in multimodal rumor detection tasks.

Observing the results, single-modality methods, such as image-only CLIP or text-only LSTM_word2vec and DEDA, generally perform worse than multimodal approaches, such as HMCAN, MTTV, which underscores the necessity of jointly leveraging both text and image features to capture complex rumor cues. Among the multimodal baselines, although methods designed for text–image consistency, such as CCN, exhibit strong competitiveness, the proposed model still achieves superior performance.

Specifically, on the Weibo dataset, the model achieves a macro accuracy of 94.9%, representing a 2.9% improvement over CCN. Notably, for the most challenging rumor category, the model reaches an F1-score of 92.2%, with a recall of 96.1%, indicating its ability to effectively reduce false negatives. Similarly, on the Twitter dataset, the model attains an extremely high precision of 97.9% for the non-rumor category.

These results indicate that the model not only captures deep semantic correlations between

text and images more accurately but also maintains robust performance across different language environments, effectively addressing the limitations of existing methods in complex contexts. Although the method achieves substantial performance improvements for the unconfirmed and rumor categories, a slight bias in recall is observed, suggesting that the model is more sensitive when identifying high-risk information.

4.3.3 Ablation Study

To verify the contribution of each module, we design the following seven ablation experiments:

1. Without Evidence Fusion: Both textual and visual evidence are removed.
2. Without Text–Image Contrast: The text–image contrastive learning module is removed.
3. Without Dual Contrast: The dual contrastive learning module is removed.
4. Without Text–Description Contrast: The text–image description contrast module is removed.
5. Without Gated Modulation: The gated fusion and adaptive feature scaling mechanisms are removed.
6. Without Forgery Feature Extraction: The forgery feature extraction module is removed.
7. Without Adaptive Feature Scaling: Only the adaptive feature scaling mechanism is removed.

The results on the Weibo and Twitter datasets are shown in Tables 3 and 4, respectively. By comparing the full model with these seven variants, the ablation study effectively validates the necessity and effectiveness of each component in the model.

Table 3

	non				rumor				unver			
	Acc	prec	rec	F1	Acc	prec	rec	F1	Acc	prec	rec	F1
w/o Dual Contrastive	93.1	96.7	97.1	96.9	92.8	87.1	89.9	92.5	95.1	93.8		
w/o Forgery Features	92.2	96.7	97.9	97.3	87.9	85.9	86.9	92.6	92.9	92.8		
w/o Gating	91.4	95.1	95.5	95.3	90.9	83.7	87.2	91.7	95.1	93.4		
w/o Evidence Fusion	91.9	98.3	92.9	95.5	88.5	86.5	87.5	91.8	96.3	94.0		
w/o Image-Text Contrastive	93.7	96.7	96.3	96.5	89.4	90.4	89.9	94.6	94.3	94.4		
w/o Text-Text Contrastive	94.1	98.3	94.2	96.2	91.1	92.1	91.6	93.8	96.0	94.9		
w/o Feature Scaling Mechanism	93.5	97.1	95.9	96.5	90.0	89.3	89.6	94.2	95.4	94.8		
ours	94.9	95.1	96.3	95.7	88.6	96.1	92.2	97.3	92.3	94.7		

Table 4

	non				rumor				unver			
	Acc	prec	rec	F1	Acc	prec	rec	F1	Acc	prec	rec	F1
w/o Dual Contrastive	92.4	93.8	98.5	96.1	87.2	84.5	85.8	96.4	94.3	95.3		
w/o Forgery Features	91.1	92.9	98.5	95.6	93.5	77.5	84.8	93.9	97.2	95.5		
w/o Gating	91.7	95.5	95.5	95.5	82.7	85.3	84.0	95.7	94.3	95.0		
w/o Evidence Fusion	91.8	96.4	94.0	95.2	80.7	87.6	84.0	96.0	93.9	94.9		

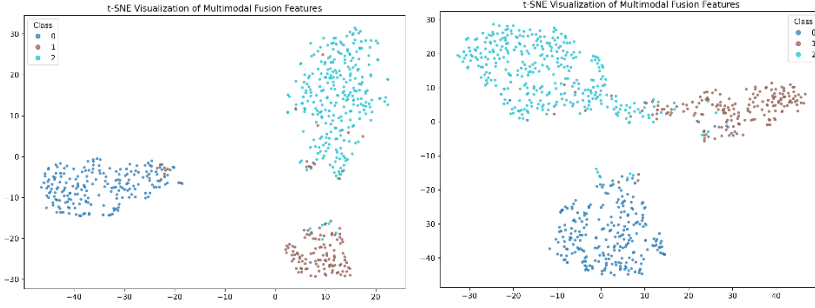
w/o Image-Text Contrastive	93.0	95.6	98.0	96.8	82.7	89.1	85.8	97.0	91.8	94.3
w/o Text-Text Contrastive	93.2	95.6	97.5	96.5	92.4	84.5	88.3	95.1	97.5	96.3
w/o Feature Scaling Mechanism	92.9	97.0	98.0	97.5	93.0	82.9	87.7	93.9	97.9	95.9
ours	94.1	97.9	95.5	96.7	85.5	91.5	88.4	96.8	95.4	96.1

The experimental results indicate that the full model achieves the best performance across all evaluation metrics, demonstrating that the modules work effectively in synergy. Among all ablation settings, removing the gated module and the image forgery feature extraction module leads to the most significant performance drops. Specifically, without the gated mechanism, the macro accuracy (Acc) on the Weibo dataset decreases by 3.5% (from 94.9% to 91.4%), and the F1-score for the rumor category is most affected, confirming the core role of the gating mechanism in regulating information flow and filtering noise. Similarly, removing the forgery feature extraction module results in a 3.0% decrease in macro accuracy on the Twitter dataset, indicating that this module is crucial for capturing image manipulation traces, especially on image-rich platforms such as Twitter. Moreover, the absence of the dual contrastive learning module (w/o dual contrast) also causes a noticeable drop in macro accuracy compared with removing a single contrast module, validating the effectiveness of jointly optimizing intra-modal and inter-modal semantic alignment. Removing the evidence fusion module similarly leads to a significant performance decline, highlighting the auxiliary role of explicit evidence information in rumor judgment. Finally, although the performance loss is relatively small, removing the adaptive feature scaling mechanism or individual contrastive modules still causes a consistent decrease in performance, indicating that these components contribute positively to model robustness and dynamic adaptability. In summary, the model achieves efficient and robust multimodal rumor detection by integrating these key mechanisms.

4.3.4 t-SNE Feature Visualization Analysis

To further verify the discriminative capability of the model during multimodal feature fusion, t-SNE was applied to visualize the fused features generated by the model on the Weibo and Twitter datasets (as shown in Figure 3). Different colors in the figure represent three classes of samples: real (blue), fake (brown), and unconfirmed (cyan).

The overall distribution shows that the model can distinguish different classes of samples well in the low-dimensional space. Real and fake samples form clearly separated clusters, indicating that the model achieves strong inter-class discriminability after multimodal feature fusion. Additionally, a small number of overlapping points exist in the transitional regions, suggesting that the model maintains flexible representations when facing modality conflicts or semantically ambiguous samples, rather than enforcing overly sharp boundaries. This continuous distribution structure is partially attributed to the introduction of the adaptive feature scaling mechanism, which makes the fused feature space smoother and more robust.



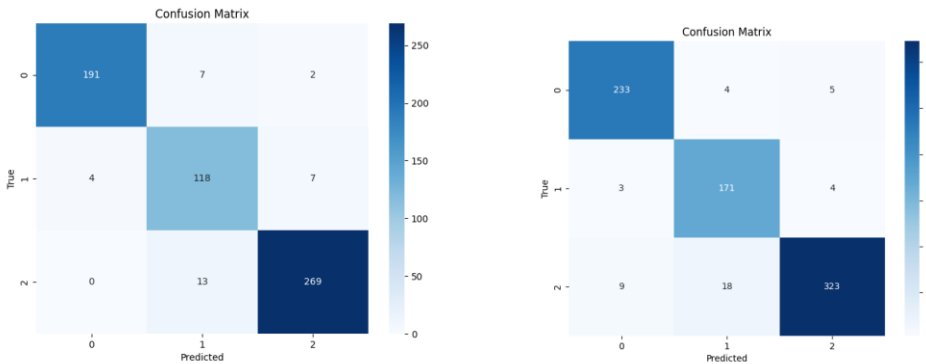
(a)twitter

(b)weibo

Figure 3

4.3.5 Error Analysis

To conduct a detailed analysis of prediction errors, we visualized the confusion matrices of the test results, as shown in Figures 4 and 5. The horizontal axis represents predicted labels, while the vertical axis represents true labels. Although the proposed model achieves the highest overall macro accuracy on both the Weibo and Twitter datasets, detailed category-level performance reveals the challenges the model faces when handling specific types of information. Macro-level comparison shows that the model performs exceptionally well on the non-rumor and unconfirmed categories across both datasets, with F1-scores generally exceeding 94%. However, for the rumor category on the Twitter dataset, the F1-score drops significantly to 87.8%, much lower than 92.2% on the Weibo dataset, indicating that identifying more covert and complex rumors on Twitter remains the primary challenge for the current model. Further analysis of the precision–recall trade-off reveals that, on the Weibo dataset, the recall of the rumor category (96.1%) is much higher than its precision (88.6%), suggesting that the model tends to classify information as rumors, resulting in a higher false positive rate (non-rumors misclassified as rumors). In contrast, the unconfirmed category exhibits high precision (97.3%) and relatively lower recall (92.3%), indicating that the model is highly cautious when confirming this type of information.



(a)twitter

(b) Weibo

Figure 4

5. Conclusion

This paper proposes a rumor detection method enhanced by external evidence and forgery features, and significantly improves model performance in rumor detection tasks by introducing a dual-contrastive learning mechanism and a gated modulation module. Extensive experiments on the MR2 dataset validate the advantages of our method in

multimodal information processing, forged image detection, and semantic alignment between text and images.

Experimental results demonstrate the critical role of integrating text and image evidence in rumor detection. Through a carefully designed evidence retrieval strategy, we identified the optimal number of evidence items, further confirming the significant impact of an appropriate amount of evidence on model performance. Insufficient evidence leads to inadequate information, while excessive evidence introduces noise, providing important guidance for future optimization of evidence selection and retrieval methods.

Our dual-contrastive learning approach fully exploits the complementarity between text and images, improving the precision of cross-modal feature alignment and enhancing model robustness when facing semantic inconsistencies or forged content. Meanwhile, the gated modulation module flexibly adjusts the fusion of text and image features, enhancing model adaptability and generalization capability.

Experimental results indicate that the introduction of adaptive feature fusion allows the model to automatically adjust fusion weights according to feature importance, effectively mitigating the negative impact of noise on performance.

In future work, we will continue to explore how more refined feature fusion and multimodal information mining methods can further enhance rumor detection performance, particularly in scenarios with extreme noise and complex environments.

6. References

- [1]Tufchi S, Yadav A, Ahmed T. A comprehensive survey of multimodal fake news detection techniques: advances, challenges, and opportunities[J]. International Journal of Multimedia Information Retrieval, 2023, 12(2): 28.
- [2]Guo X, Liu X, Ren Z, et al. Hierarchical fine-grained image forgery detection and localization[C]//Proceedings of the IEEE/CVF conference on computer vision and pattern recognition. 2023: 3155-3165.
- [3]Wang B, Wu X, Tang Y, et al. Frequency domain filtered residual network for deepfake detection[J]. Mathematics, 2023, 11(4): 816.
- [4]Wang L, Zhang C, Xu H, et al. Cross-modal contrastive learning for multimodal fake news detection[C]//Proceedings of the 31st ACM international conference on multimedia. 2023: 5696-5704.
- [5]Li J, Bin Y, Zou J, et al. Cross-modal consistency learning with fine-grained fusion network for multimodal fake news detection[C]//Proceedings of the 5th ACM International Conference on Multimedia in Asia. 2023: 1-7.
- [6] Kwon S, Cha M, Jung K, et al. Prominent features of rumor propagation in online social media[C]//2013 IEEE 13th international conference on data mining. IEEE, 2013: 1103-1108.
- [7] Ma J, Gao W, Mitra P, et al. Detecting rumors from microblogs with recurrent neural networks[J]. 2016.
- [8] Chen T, Li X, Yin H, et al. Call attention to rumors: Deep attention based recurrent neural networks for early rumor detection[C]//Pacific-Asia conference on knowledge discovery and

data mining. Cham: Springer International Publishing, 2018: 40-52.

[9] Alkhodair S A, Ding S H H, Fung B C M, et al. Detecting breaking news rumors of emerging topics in social media[J]. *Information Processing & Management*, 2020, 57(2): 102018.

[10] Luvembe A M, Li W, Li S, et al. Dual emotion based fake news detection: A deep attention-weight update approach[J]. *Information Processing & Management*, 2023, 60(4): 103354.

[11] Xu F, Sheng V S, Wang M. Near real-time topic-driven rumor detection in source microblogs[J]. *Knowledge-Based Systems*, 2020, 207: 106391.

[12] Cao J, Qi P, Sheng Q, et al. Exploring the role of visual content in fake news detection[J]. *Disinformation, Misinformation, and Fake News in Social Media: Emerging Research Challenges and Opportunities*, 2020: 141-161.

[13] Qi P, Cao J, Yang T, et al. Exploiting multi-domain visual information for fake news detection[C]//2019 IEEE international conference on data mining (ICDM). IEEE, 2019: 518-527.

[14] Huang Y, Sun L. FakeGPT: fake news generation, explanation and detection of large language models[J]. arXiv preprint arXiv:2310.05046, 2023.

[15] Zhang X, Gao W. Towards llm-based fact verification on news claims with a hierarchical step-by-step prompting method[J]. arXiv preprint arXiv:2310.00305, 2023.

[16] Wang Y, Ma F, Jin Z, et al. Eann: Event adversarial neural networks for multi-modal fake news detection[C]//Proceedings of the 24th acm sigkdd international conference on knowledge discovery & data mining. 2018: 849-857.

[17] Nguyen D M, Do T H, Calderbank R, et al. Fake news detection using deep markov random fields[C]//Proceedings of the 2019 Conference of the North American Chapter of the Association for Computational Linguistics: Human Language Technologies, Volume 1 (Long and Short Papers). 2019: 1391-1400.

[18] Kirchknopf A, Slijepčević D, Zeppelzauer M. Multimodal detection of information disorder from social media[C]//2021 International conference on content-based multimedia indexing (CBMI). IEEE, 2021: 1-4.

[19] Luvembe A M, Li W, Li S, et al. CAF-ODNN: Complementary attention fusion with optimized deep neural network for multimodal fake news detection[J]. *Information Processing & Management*, 2024, 61(3): 103653.

[20] Liu X, Pang M, Li Q, et al. MVACLNet: A multimodal virtual augmentation contrastive learning network for rumor detection[J]. *Algorithms*, 2024, 17(5): 199.

[21] Zhou X, Wu J, Zafarani R. : Similarity-aware multi-modal fake news detection[C]//Pacific-Asia Conference on knowledge discovery and data mining. Cham: Springer International Publishing, 2020: 354-367.

[22] Xue J, Wang Y, Tian Y, et al. Detecting fake news by exploring the consistency of

multimodal data[J]. *Information Processing & Management*, 2021, 58(5): 102610.

[23] Abdelnabi S, Hasan R, Fritz M. Open-domain, content-based, multi-modal fact-checking of out-of-context images via online resources[C]//Proceedings of the IEEE/CVF conference on computer vision and pattern recognition. 2022: 14940-14949.

[24] Zhang X, Dadkhah S, Weismann A G, et al. Multimodal fake news analysis based on image-text similarity[J]. *IEEE Transactions on Computational Social Systems*, 2023, 11(1): 959-972.

[25] Wu K, Cao D. Evidence-aware multimodal Chinese social media rumor detection[C]//ICASSP 2024-2024 IEEE International Conference on Acoustics, Speech and Signal Processing (ICASSP). IEEE, 2024: 8376-8380.

[26] Wu Y, Sun J, Yuan X, et al. Dual-channel early rumor detection based on factual evidence[J]. *Expert Systems with Applications*, 2024, 238: 121928.

[27] Huang X, Ma T, Rong H, et al. Dual evidence enhancement and text-image similarity awareness for multimodal rumor detection[J]. *Engineering Applications of Artificial Intelligence*, 2025, 153: 110845.

[28] Li J, Li D, Xiong C, et al. Blip: Bootstrapping language-image pre-training for unified vision-language understanding and generation[C]//International conference on machine learning. PMLR, 2022: 12888-12900.

[29] Hu X, Guo Z, Chen J, et al. Mr2: A benchmark for multimodal retrieval-augmented rumor detection in social media[C]//Proceedings of the 46th international ACM SIGIR conference on research and development in information retrieval. 2023: 2901-2912.

[30] Radford A, Kim J W, Hallacy C, et al. Learning transferable visual models from natural language supervision[C]//International conference on machine learning. PmLR, 2021: 8748-8763.

[31] Wang B, Feng Y, Xiong X, et al. Multi-modal transformer using two-level visual features for fake news detection[J]. *Applied Intelligence*, 2023, 53(9): 10429-10443.

[32] Qian S, Wang J, Hu J, et al. Hierarchical multi-modal contextual attention network for fake news detection[C]//Proceedings of the 44th international ACM SIGIR conference on research and development in information retrieval. 2021: 153-162.